OL Organic Letters

pubs.acs.org/OrgLett

Letter

A Heterogeneous Iridium Catalyst for the Hydroboration of Pyridines

Jessica Rodriguez and Matthew P. Conley*

Cite This: *Org. Lett.* 2022, 24, 4680−4683

Read Online

ACCESS | Metrics & More | Article Recommendations | Supporting Information

ABSTRACT: Sulfated zirconium oxide (SZO) capped with silylium-like ions reacts with (cod)Ir(py)Cl (cod = 1,5-cyclooctadiene; py = pyridine) to form [Ir(cod)py][SZO] (**1**) and Me_3SiCl. **1** can also be formed in reactions of phosphonium functionalized SZO and $[Ir(cod)(OSi(O^tBu)_3]_2$, which forms $[Ir(cod)P(^tBu)_2Ph][SZO]$ (**2**), followed by reaction with pyridine to form **1**. FTIR and $^{15}N\{^1H\}$ MAS NMR spectroscopy are consistent with coordination of pyridine in **1** to an electrophilic iridium. **1** is moderately active in the dearomative hydroboration of pyridine. The primary product of this reaction is 1,2-dihydropyridine, which converts to the 1,4-dihydropyridine product at long reaction times. **1** catalyzes the dearomative hydroboration of a variety of substituted pyridines and is also reactive toward pyrazines and *N*-methylimidazole.

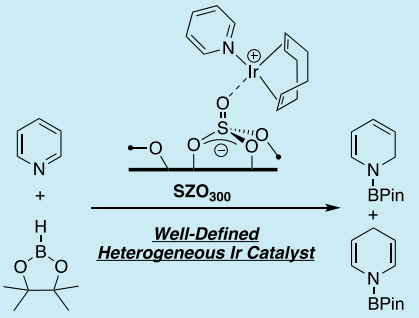

Reactions of pyridines with silanes or boranes in the presence of a catalyst results in dearomatized heterocyclic products that are intermediates for common motifs in natural products and pharmaceutically active small molecules.[1] These reactions can form either the 1,2- or 1,4-dihydropyridine product. Figure 1 shows simplified mechanistic steps that form

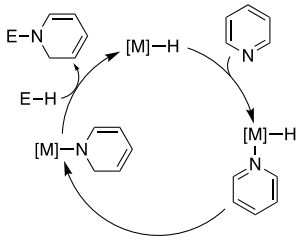

Figure 1. Simplified mechanism for the dearomatization of pyridines with a generic metal hydride (E = SiR_3, $B(OR)_2$).

the 1,2-dihydropyridine. A metal hydride coordinates pyridine, which then undergoes C═N insertion to generate the dearomatized metal amide. Exogeneous silane or borane reacts with the metal amide to release the silylated or hydroborated heterocycle and regenerates the metal hydride.

Alkaline earths,[2] lanthanides,[3] actinides,[4] first-row transition metals,[5] bimetallics,[6] rhenium,[7] rhodium,[8] ruthenium,[9] and metal organic frameworks[10] catalyze or mediate the reaction shown in Figure 1. In addition, simple alkoxides[11] and main group Lewis acids[12] also form dearomatized products in the presence of pyridine and pinacolborane (HBPin).

Access to heterogeneous catalysts that show similar activity and selectivity profiles to homogeneous catalysts is a long-standing challenge.[13] In addition, generation of heterogeneous catalysts for fine chemical synthesis could influence the design of materials that are crucial for more efficient catalysis of small molecules under flow conditions.[14] This paper describes the synthesis and generation of electrophilic Ir sites supported on sulfated zirconium oxide partially dehydroxylated at 300 °C (SZO_{300}) that are reactive in the hydroboration of pyridine.

$[Ir(cod)py][SZO_{300}]$ (**1**) was synthesized using one of the two routes shown in Scheme 1. The reaction of $[^tBu_2PhPH][SZO_{300}]$[15] with $[Ir(cod)(OSi(O^tBu)_3]_2$[16] forms $[Ir(cod)P(^tBu)_2Ph][SZO_{300}]$ (**2**) and $HOSi(O^tBu)_3$ (0.095 mmol/g). The $^{31}P\{^1H\}$ MAS NMR of **1** contains a signal at 37 ppm that is 12 ppm downfield from the $^{31}P\{^1H\}$ MAS spectrum of $[(^tBu)_2PhPH][SZO_{300}]$ (Figure S4). Reactions of **2** with free pyridine result in quantitative displacement of P^tBu_2Ph and the formation of $[Ir(cod)py][SZO_{300}]$ (**1**).

A more direct synthesis of **1** is from (cod)IrCl(py)[17] and $[Me_3Si][SZO_{300}]$. In this reaction the silylium-like Me_3Si^+ fragment[18] supported on the weakly coordinating SZO surface[19] abstracts the halide from (cod)IrCl(py) to form **1** and Me_3SiCl (0.11 mmol/g).[20] Inductively coupled plasma−optical emission spectrometry (ICP-OES) analysis of digested **1** gives 0.083 ± 0.001 $mmol_{Ir}$ g^{-1}, which is close to the expected 1:1 ratio of Me_3SiCl:Ir expected in the halide abstraction reaction. Among the advantages of the halide abstraction methodology is more efficient ^{15}N labeling in **1** using (cod)Ir(^{15}N-py)Cl to form **1**-^{15}**N**. Figure 2a shows the FTIR spectrum of **1** and **1**-^{15}**N**. These spectra contain strong

Received: June 1, 2022
Published: June 16, 2022

Scheme 1. Synthesis of 1

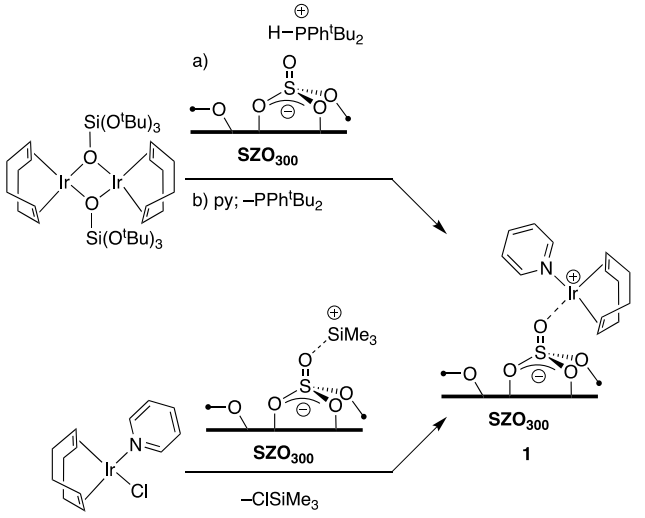

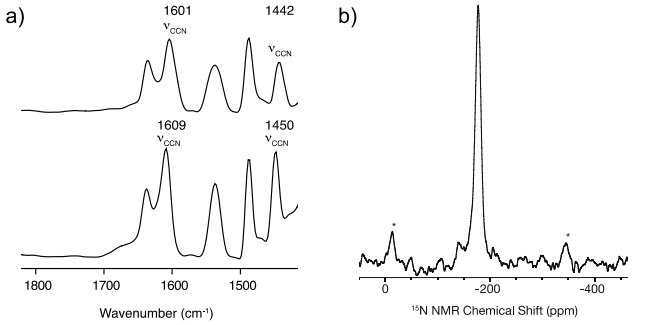

Figure 2. Expansion of the FTIR of **1** (bottom) and **1**-^{15}**N** (top) (a). A full FTIR spectrum is shown in Figure S2. ^{15}N{^{1}H} CPMAS NMR of **1**-^{15}**N** (b). (* = spinning side band).

$\nu_{C=C}$ stretches at 1609 and 1450 cm^{-1} for **1**, which shift to 1601 and 1442 cm^{-1} in **1**-^{15}**N**. The ^{13}C CPMAS NMR spectrum of **1** contains signals at 153, 140, and 128 ppm from *o*-$C_{pyridine}$, *m*-$C_{pyridine}$, and *p*-$C_{pyridine}$, respectively. This spectrum also contains signals at 34 and 29 for the cod ligand. The ^{15}N{^{1}H} CPMAS NMR of **1**-^{15}**N** is shown in Figure 2b and contains a signal at −179 ppm (referenced to CH_3NO_2 at 0 ppm). This value is shifted significantly from free pyridine (δ = −63 ppm). The NMR and FTIR data are consistent with pyridine coordination to an electrophilic iridium.[21,22]

Figure 3 shows the conversion of pyridine (**3**) in the presence of 2.5 equiv of HBPin and 1 mol % **1** to generate mixtures of hydroborated products. Monitoring this reaction over time (Figure 3b) shows that **3a** forms without a noticeable induction period and is formed in preference to **3b**. This result indicates that **3a** is the primary product of this reaction. However, **3b** is favored at longer reaction times. After 3 days at 85 °C in C_6D_6 **1** gives a 77% yield of hydroboration products, favoring the 1,4-hydroboration product **3b** over **3a** (**3a**:**3b** = 1:10).

Removal of **1** by filtration after 12 h results in 18% conversion to **3a** and **3b** (**3a**:**3b** = 1:1). Heating this mixture at 85 °C for 1 week does not result in further conversion of pyridine nor a change in the **3a**:**3b** ratio. This result indicates that catalytically competent homogeneous Ir species do not desorb from SZO_{300} during catalysis and that **1** is likely responsible for the isomerization of **3a** to **3b**.

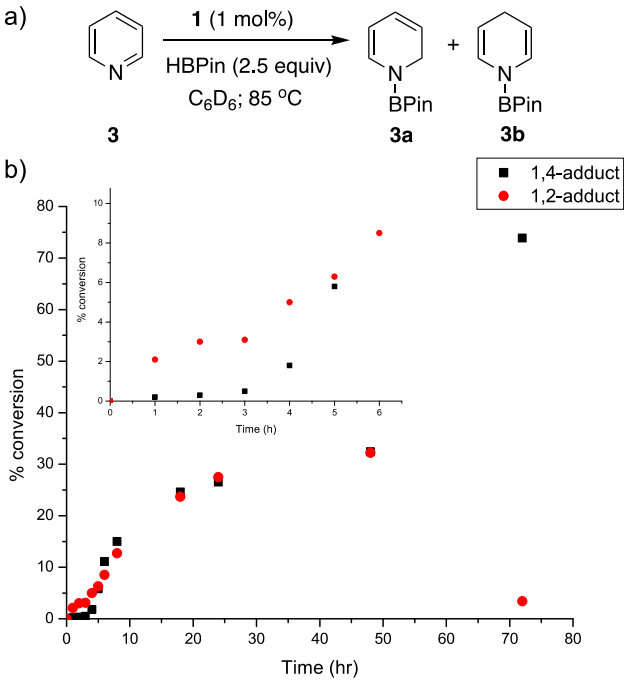

Figure 3. Reaction of pyridine (**3**) with HBPin and **1** to form **3a** and **3b** (a). Conversion versus time plot showing the product selectivity over 3 days (b). The inset shows conversion to **3a** and **3b** at low conversion (<10%) of pyridine.

Heating SZO_{300}, pyridine, and HBPin in C_6D_6 at 85 °C for 3 days results in low conversion (3%) of pyridine to a 1:2 mixture of **3a** and **3b**, showing that SZO_{300} is not an effective catalyst for this reaction. However, the support is critical for clean hydroboration chemistry. Mixtures of $[(cod)IrCl]_2$ and AgOTf in the presence of pyridine and HBPin also result in only 4% yield of **3b** after 3 days at 85 °C in C_6D_6.

Figure 4 shows the scope of the hydroboration reaction with various substitution patterns on the pyridine ring. The reactivity trends shown in Figure 4 are complementary to many of the homogeneous catalysts mentioned above. Monosubstituted pyridines tend to react to give mixtures of 1,2- and 1,4-hydroboration products. 2-Picoline (**4**) and 4-picoline (**10**) react to give a 1:10 ratio in favor of the 1,4-hydroboration product in high yield. However, 3-methoxypyridine (**5**), 3-picoline (**6**), 4-phenylpyridine (**8**), and 4-^{t}Bu-pyridine (**9**) give 1,2-borylation as the only product in the reaction mixture. 3-Phenylpyridine (**7**) reacts with **1** to give a mixture containing both isomers that are products of 1,2-hydroboration and the 1,4-hydroboration product, which is common for this substrate. Disubstituted pyridines all favor the formation of the 1,2-hydroboration product. Acridine (**14**) and quinoline (**15**) are cleanly hydroborated under these conditions in high yield. 2-Bromopyridine, 2-methoxypyridine, 2-phenylpyridine, and 2,5-dichloropydine do not produce dearomatization products under these conditions.

Related reactivity of **1** in hydroboration of heterocycles is summarized in Scheme 2. Pyrazine (**16**) reacts with **1** in the presence of HBPin to form *N*,*N*′-diboryl-1,2,3,4-tetrahydropyrazine in high yield. 2-Methoxypyrazine (**17**) reacts with **1** and HBPin to give the *N*,*N*′-diboryl-2-methoxy-1,2-dihydropyrazine product. **1** also catalyzes the hydroboration of *N*-methylimidazole (**18**) to give the hydroborated product in good yield in only 2 h.

https://doi.org/10.1021/acs.orglett.2c01859
Org. Lett. 2022, 24, 4680−4683

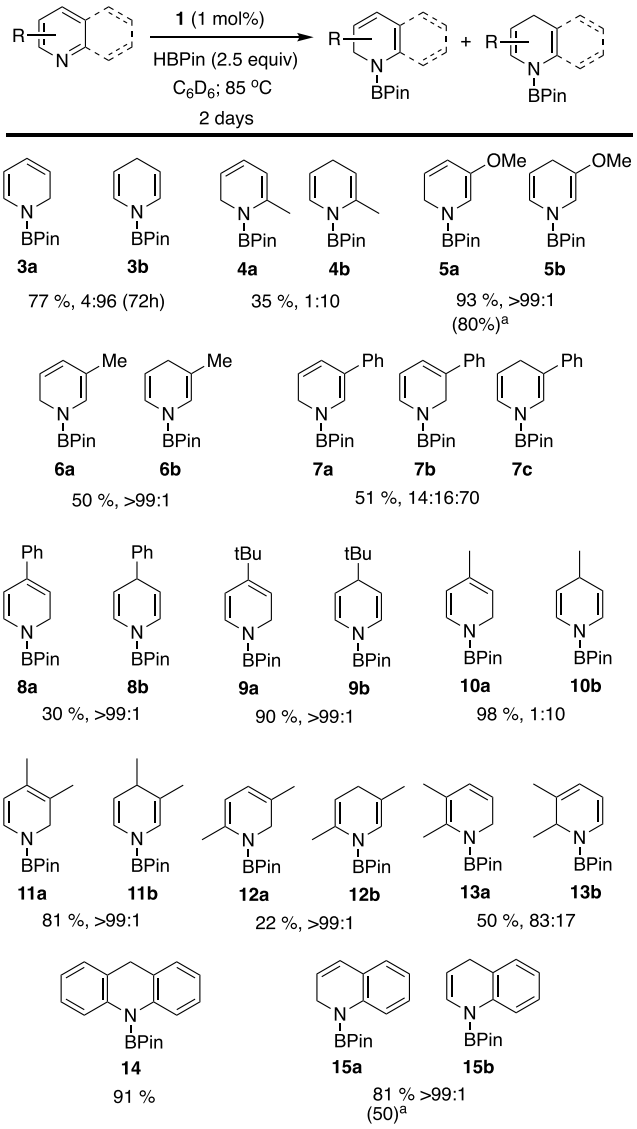

Figure 4. Scope for the dearomative hydroboration of pyridines. [a]Isolated yield.

Scheme 2. Reactivity of Pyrazines and *N*-Methylimidazole with HBPin and Catalytic 1

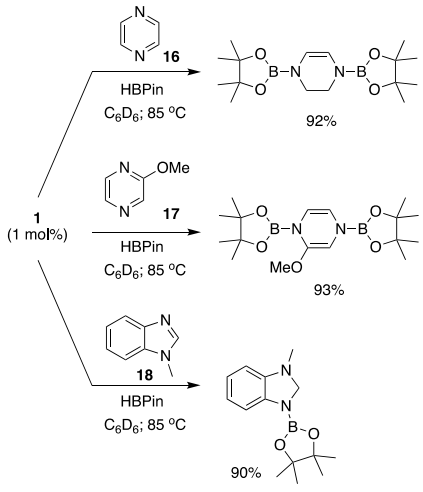

Well-defined iridium sites supported on SZO_{300} are accessible using two complementary synthetic methods. FTIR and ^{15}N MAS NMR spectroscopy are consistent with **1** containing an electrophilic iridium site. **1** is active in the dearomative hydroboration of pyridines and shows complementary reactivity toward pyrazines and *N*-methylimidazole. **1** shows comparable turnover numbers to the homogeneous catalysts referenced above. Clear mechanistic information about how **1** catalyzes this reaction will require more study, but **1** probably forms an iridium boryl hydride intermediate that could react with pyridine either through a mechanism similar to that shown in Figure 1 or through reaction of the pyridyl nitrogen with the Ir-BPin. However, there are no C−H borylation products observed when using **1** under these conditions.[23] Finally, the halide abstraction methodology used to generate **1** may constitute a general strategy to form well-defined heterogeneous catalysts from readily available inorganic precursors that could form active sites for a variety of reactions important in small-molecule synthesis.

■ ASSOCIATED CONTENT

Supporting Information

The Supporting Information is available free of charge at https://pubs.acs.org/doi/10.1021/acs.orglett.2c01859.

Experimental methods, solid-state NMR spectra, solution NMR spectra of products shown in Table 1 (PDF)

■ AUTHOR INFORMATION

Corresponding Author

Matthew P. Conley − *Department of Chemistry, University of California, Riverside, California 92521, United States;* orcid.org/0000-0001-8593-5814; Email: matthew.conley@ucr.edu

Author

Jessica Rodriguez − *Department of Chemistry, University of California, Riverside, California 92521, United States*

Complete contact information is available at: https://pubs.acs.org/10.1021/acs.orglett.2c01859

Author Contributions

The manuscript was written through contributions of both authors.

Notes

The authors declare no competing financial interest.

■ ACKNOWLEDGMENTS

M.P.C. is a member of the UCR Center for Catalysis. This work was supported by the National Science Foundation (CHE-2101582).

■ REFERENCES

(1) Park, S.; Chang, S. Catalytic Dearomatization of N-Heteroarenes with Silicon and Boron Compounds. *Angew. Chem., Int. Ed.* **2017**, *56*, 7720−7738.

(2) (a) Arrowsmith, M.; Hill, M. S.; Hadlington, T.; Kociok-Köhn, G.; Weetman, C. Magnesium-Catalyzed Hydroboration of Pyridines. *Organometallics* **2011**, *30*, 5556−5559. (b) Intemann, J.; Lutz, M.; Harder, S. Multinuclear Magnesium Hydride Clusters: Selective Reduction and Catalytic Hydroboration of Pyridines. *Organometallics* **2014**, *33*, 5722−5729.

(3) Dudnik, A. S.; Weidner, V. L.; Motta, A.; Delferro, M.; Marks, T. J. Atom-efficient regioselective 1,2-dearomatization of functionalized pyridines by an earth-abundant organolanthanide catalyst. *Nat. Chem.* **2014**, *6*, 1100−1107.
(4) Liu, H.; Khononov, M.; Eisen, M. S. Catalytic 1,2-Regioselective Dearomatization of N-Heteroaromatics via a Hydroboration. *ACS Catal.* **2018**, *8*, 3673−3677.
(5) (a) Zhang, F.; Song, H.; Zhuang, X.; Tung, C.-H.; Wang, W. Iron-Catalyzed 1,2-Selective Hydroboration of N-Heteroarenes. *J. Am. Chem. Soc.* **2017**, *139*, 17775−17778. (b) Tamang, S. R.; Singh, A.; Unruh, D. K.; Findlater, M. Nickel-Catalyzed Regioselective 1,4-Hydroboration of N-Heteroarenes. *ACS Catal.* **2018**, *8*, 6186−6191. (c) Liu, J.; Chen, J.-Y.; Jia, M.; Ming, B.; Jia, J.; Liao, R.-Z.; Tung, C.-H.; Wang, W. Ni−O Cooperation versus Nickel(II) Hydride in Catalytic Hydroboration of N-Heteroarenes. *ACS Catal.* **2019**, *9*, 3849−3857. (d) Lortie, J. L.; Dudding, T.; Gabidullin, B. M.; Nikonov, G. I. Zinc-Catalyzed Hydrosilylation and Hydroboration of N-Heterocycles. *ACS Catal.* **2017**, *7*, 8454−8459. (e) Wang, X.; Zhang, Y.; Yuan, D.; Yao, Y. Regioselective Hydroboration and Hydrosilylation of N-Heteroarenes Catalyzed by a Zinc Alkyl Complex. *Org. Lett.* **2020**, *22*, 5695−5700. (f) Ghosh, P.; Jacobi von Wangelin, A. Manganese-Catalyzed Hydroborations with Broad Scope. *Angew. Chem., Int. Ed.* **2021**, *60*, 16035−16043.
(6) Yu, H.-C.; Islam, S. M.; Mankad, N. P. Cooperative Heterobimetallic Substrate Activation Enhances Catalytic Activity and Amplifies Regioselectivity in 1,4-Hydroboration of Pyridines. *ACS Catal.* **2020**, *10*, 3670−3675.
(7) Donnelly, L. J.; Parsons, S.; Morrison, C. A.; Thomas, S. P.; Love, J. B. Synthesis and structures of anionic rhenium polyhydride complexes of boron−hydride ligands and their application in catalysis. *Chem. Sci.* **2020**, *11*, 9994−9999.
(8) Oshima, K.; Ohmura, T.; Suginome, M. Regioselective Synthesis of 1,2-Dihydropyridines by Rhodium-Catalyzed Hydroboration of Pyridines. *J. Am. Chem. Soc.* **2012**, *134*, 3699−3702.
(9) Kaithal, A.; Chatterjee, B.; Gunanathan, C. Ruthenium-Catalyzed Regioselective 1,4-Hydroboration of Pyridines. *Org. Lett.* **2016**, *18*, 3402−3405.
(10) (a) Ji, P.; Sawano, T.; Lin, Z.; Urban, A.; Boures, D.; Lin, W. Cerium-Hydride Secondary Building Units in a Porous Metal−Organic Framework for Catalytic Hydroboration and Hydrophosphination. *J. Am. Chem. Soc.* **2016**, *138*, 14860−14863. (b) Ji, P.; Feng, X.; Veroneau, S. S.; Song, Y.; Lin, W. Trivalent Zirconium and Hafnium Metal−Organic Frameworks for Catalytic 1,4-Dearomative Additions of Pyridines and Quinolines. *J. Am. Chem. Soc.* **2017**, *139*, 15600−15603.
(11) (a) Jeong, E.; Heo, J.; Park, S.; Chang, S. Alkoxide-Promoted Selective Hydroboration of N-Heteroarenes: Pivotal Roles of in situ Generated BH3 in the Dearomatization Process. *Chem.−Eur. J.* **2019**, *25*, 6320−6325. (b) Rauch, M.; Ruccolo, S.; Parkin, G. Synthesis, Structure, and Reactivity of a Terminal Magnesium Hydride Compound with a Carbatrane Motif, [TismPriBenz]MgH: A Multifunctional Catalyst for Hydrosilylation and Hydroboration. *J. Am. Chem. Soc.* **2017**, *139*, 13264−13267. (c) Mukherjee, D.; Shirase, S.; Spaniol, T. P.; Mashima, K.; Okuda, J. Magnesium hydrido-triphenylborate [Mg(thf)6][HBPh3]2: a versatile hydroboration catalyst. *Chem. Commun.* **2016**, *52*, 13155−13158. (d) Fohlmeister, L.; Stasch, A. Ring-Shaped Phosphinoamido-Magnesium-Hydride Complexes: Syntheses, Structures, Reactivity, and Catalysis. *Chem.−Eur. J.* **2016**, *22*, 10235−10246. (e) Liu, X.; Li, B.; Hua, X.; Cui, D. 1,2-Hydroboration of Pyridines by Organomagnesium. *Org. Lett.* **2020**, *22*, 4960−4965.
(12) (a) Fan, X.; Zheng, J.; Li, Z. H.; Wang, H. Organoborane Catalyzed Regioselective 1,4-Hydroboration of Pyridines. *J. Am. Chem. Soc.* **2015**, *137*, 4916−4919. (b) Rao, B.; Chong, C. C.; Kinjo, R. Metal-Free Regio- and Chemoselective Hydroboration of Pyridines Catalyzed by 1,3,2-Diazaphosphenium Triflate. *J. Am. Chem. Soc.* **2018**, *140*, 652−656. (c) Jeong, J.; Heo, J.; Kim, D.; Chang, S. NHC-Catalyzed 1,2-Selective Hydroboration of Quinolines. *ACS Catal.* **2020**, *10*, 5023−5029.
(13) (a) Cui, X.; Li, W.; Ryabchuk, P.; Junge, K.; Beller, M. Bridging homogeneous and heterogeneous catalysis by heterogeneous single-metal-site catalysts. *Nature Catalysis* **2018**, *1*, 385−397. (b) Copéret, C.; Comas-Vives, A.; Conley, M. P.; Estes, D. P.; Fedorov, A.; Mougel, V.; Nagae, H.; Núñez-Zarur, F.; Zhizhko, P. A. Surface Organometallic and Coordination Chemistry toward Single-Site Heterogeneous Catalysts: Strategies, Methods, Structures, and Activities. *Chem. Rev.* **2016**, *116*, 323−421. (c) Stalzer, M.; Delferro, M.; Marks, T. Supported Single-Site Organometallic Catalysts for the Synthesis of High-Performance Polyolefins. *Catal. Lett.* **2015**, *145*, 3−14. (d) Guzman, J.; Gates, B. C. Supported molecular catalysts: metal complexes and clusters on oxides and zeolites. *Dalton Trans.* **2003**, 3303−3318.
(14) (a) Yu, T.; Ding, Z.; Nie, W.; Jiao, J.; Zhang, H.; Zhang, Q.; Xue, C.; Duan, X.; Yamada, Y. M. A.; Li, P. Recent Advances in Continuous-Flow Enantioselective Catalysis. *Chem.−Eur. J.* **2020**, *26*, 5729−5747. (b) Zhao, D.; Ding, K. Recent Advances in Asymmetric Catalysis in Flow. *ACS Catal.* **2013**, *3*, 928−944.
(15) Rodriguez, J.; Culver, D. B.; Conley, M. P. Generation of Phosphonium Sites on Sulfated Zirconium Oxide: Relationship to Brønsted Acid Strength of Surface − OH Sites. *J. Am. Chem. Soc.* **2019**, *141*, 1484−1488.
(16) Héroguel, F.; Gebert, D.; Detwiler, M. D.; Zemlyanov, D. Y.; Baudouin, D.; Copéret, C. Dense and narrowly distributed silica-supported rhodium and iridium nanoparticles: Preparation via surface organometallic chemistry and chemisorption stoichiometry. *J. Catal.* **2014**, *316*, 260−269.
(17) Zassinovich, G.; Mestroni, G.; Camus, A. Diolefinic complexes of rhodium(I) and iridium(I) with nitrogen-containing ligands. *J. Organomet. Chem.* **1975**, *91*, 379−388.
(18) Culver, D. B.; Conley, M. P. Activation of C−F Bonds by Electrophilic Organosilicon Sites Supported on Sulfated Zirconia. *Angew. Chem., Int. Ed.* **2018**, *57*, 14902−14905.
(19) Witzke, R. J.; Chapovetsky, A.; Conley, M. P.; Kaphan, D. M.; Delferro, M. Non-Traditional Catalyst Supports in Surface Organometallic Chemistry. *ACS Catal.* **2020**, *10*, 11822−11840.
(20) Gao, J.; Dorn, R. W.; Laurent, G. P.; Perras, F. A.; Rossini, A. J.; Conley, M. P. A Heterogeneous Palladium Catalyst for the Polymerization of Olefins Prepared by Halide Abstraction Using Surface R3Si+ Species. *Angew. Chem., Int. Ed.* **2022**, e202117279.
(21) Gunther, W. R.; Michaelis, V. K.; Griffin, R. G.; Román-Leshkov, Y. Interrogating the Lewis Acidity of Metal Sites in Beta Zeolites with 15N Pyridine Adsorption Coupled with MAS NMR Spectroscopy. *J. Phys. Chem. C* **2016**, *120*, 28533−28544.
(22) Zaki, M. I.; Hasan, M. A.; Al-Sagheer, F. A.; Pasupulety, L. In situ FTIR spectra of pyridine adsorbed on SiO2−Al2O3, TiO2, ZrO2 and CeO2: general considerations for the identification of acid sites on surfaces of finely divided metal oxides. *Colloids Surf., A* **2001**, *190*, 261−274.
(23) Recent Review: Wright, J. S.; Scott, P. J. H.; Steel, P. G. Iridium-Catalysed C−H Borylation of Heteroarenes: Balancing Steric and Electronic Regiocontrol. *Angew. Chem., Int. Ed.* **2021**, *60*, 2796−2821.

https://doi.org/10.1021/acs.orglett.2c01859
Org. Lett. 2022, 24, 4680−4683